

Solitonic Spin-Liquid State Due to the Violation of the Lifshitz Condition in Fe_{1+y}Te

Ph. Materne,¹ C. Koz,² U. K. Rößler,³ M. Doerr,¹ T. Goltz,¹ H. H. Klauss,¹ U. Schwarz,² S. Wirth,² and S. Rößler^{2,*}

¹*Institut für Festkörperphysik, Technische Universität Dresden, 01062 Dresden, Germany*

²*Max Planck Institute for Chemical Physics of Solids, Nöthnitzer Straße 40, 01187 Dresden, Germany*

³*IFW Dresden, Postfach 270016, 01171 Dresden, Germany*

(Received 10 August 2015; published 21 October 2015)

A combination of phenomenological analysis and Mössbauer spectroscopy experiments on the tetragonal Fe_{1+y}Te system indicates that the magnetic ordering transition in compounds with higher Fe excess, $y \geq 0.11$, is unconventional. Experimentally, a liquidlike magnetic precursor with quasistatic spin order is found from significantly broadened Mössbauer spectra at temperatures above the antiferromagnetic transition. The incommensurate spin-density wave order in Fe_{1+y}Te is described by a magnetic free energy that violates the weak Lifshitz condition in the Landau theory of second-order transitions. The presence of multiple Lifshitz invariants provides the mechanism to create multidimensional, twisted, and modulated solitonic phases.

DOI: [10.1103/PhysRevLett.115.177203](https://doi.org/10.1103/PhysRevLett.115.177203)

PACS numbers: 75.10.-b, 74.70.Xa, 75.30.Kz, 76.80.+y

Complex ordering in solids is often associated with precursor phenomena. In the nonordered state, some features of the true long-range order (LRO) are already present locally or temporarily. The onset of these precursors above the transition is usually not distinguished by a clear thermodynamic anomaly. Some examples are the normal state (pseudogap) in doped cuprates [1] and heavy fermion superconductors [2], magnetic polarons in the colossal magnetoresistive manganites [3] and EuB_6 , [4] blue phases in chiral nematic liquid crystals [5], and precursor phenomena in noncentrosymmetric helimagnets [6–8].

Here, we argue that similar precursor phenomena as in the noncentrosymmetric liquid crystals and magnets exist in a great number of other condensed matter systems. In particular, magnetic ordering into modulated states provides a rich variety of systems where such effects should be observable [9–11]. Phenomenological Landau theory is a secure guide for identifying candidate systems for such effects. If the order parameter can be rotated by the presence of several twisting terms, known as Lifshitz invariants, in the phenomenological free-(Landau-Ginzburg)-energy, a continuous phase transition into a homogeneously ordered phase is impossible [12]. Ordering under the influence of such twisting terms is described by Dzyaloshinskii models [9]. Corresponding systems can display liquidlike mesophases as precursors, which are composed of multidimensional, localized (solitonic) states [13] that can be fluctuatingly nucleated before LRO is established [6,7].

In this Letter, we identify one interesting example for such a magnetically modulated precursor. The tetragonal Fe_{1+y}Te ($y = 0.13$ and 0.15) is a parent to one class of Fe-based superconductors which undergoes a magnetic ordering transition at low temperatures into a modulated antiferromagnetic state [14–18] which has been described as continuous. However, it does not obey the standard

Landau theory. Using symmetry arguments, we have constructed the corresponding Dzyaloshinskii theory and show that it violates the weak Lifshitz criterion [12]. This motivates the search for a magnetic precursor state similar to those found in chiral helimagnets [6–8]. The Fe-based material is ideally suited for identifying such quasistatic magnetic states above the long-range ordering temperature, as the hyperfine-field distribution observable in the Mössbauer spectroscopy reflects the inhomogeneous spin-state established in these liquidlike spin structures. This precursor state signals an exotic magnetic ordering in Fe chalcogenides within an intermediate temperature range.

The nonsuperconducting parent compounds of Fe-based superconductors are interesting systems on their own, as they show a complex interplay of magnetic and structural phase transitions, which indicate a competition of several ordering phenomena. Among the different families of Fe-based superconductors, the chalcogenides with “11” structure can be considered as reference systems owing to their representative and simple crystal structure. Fe_{1+y}Te has a particularly rich phase diagram [15,17–19], and neutron scattering studies [14,20–24] on these materials have identified some peculiar properties. The propagation vector along $(0, \pi)$ at low Fe excess suggests that nesting does not play a crucial role (see, e.g., Ref. [25]) but demonstrates the existence of a microscopic mechanism for the formation of an antiferromagnetic type of order similar to a spin-density wave (SDW). The observed ordered moment in Fe_{1+y}Te is significantly large in comparison to the parent pnictides. Fe_{1+y}Te also displays an unconventional, temperature-enhanced magnetism [22]. The low-temperature crystal and magnetic structures, as well as the commensurability of the propagation vector in Fe_{1+y}Te depend on the occupancy of the excess Fe (y) in the crystallographic $2c$ site within the $P4/nmm$ space group. Compounds of higher doping

$y \geq 0.11$ undergo a continuous transition [15,16] into an incommensurate, and possibly helical, magnetic state [26]. The onset temperature of this LRO increases with Fe content: $T_N(y = 0.11) = 57$ K, and $T_N(y = 0.15) = 63$ K. For $0.11 < y \leq 0.13$, this is followed by a transition into a collinear SDW phase by a first-order magnetostructural phase transition, i.e., a lock-in transition takes place at a temperature $T_l < T_N$ [15].

The experimentally observed continuous magnetic ordering into an incommensurate modulated state in Fe_{1+y}Te for $y \geq 0.11$ must obey a generalized (nonlocal) Landau theory [10]. Considering the propagation vector $\mathbf{q} \sim (0, \Delta, 1/2)$ with $\Delta \approx 0.38$ to 0.45 reported for Fe_{1+y}Te with $y \geq 0.11$ [14,20], the ordering modes are SDWs with sets of propagation vectors that have the same symmetry as \mathbf{q} , around a base mode Φ , with propagation vector \mathbf{q}_0 [9]. The free energy density is expanded in the \mathbf{q} -depending Φ and its gradients. The leading square term in order parameter (OP) components is

$$w_L = \Phi^* (\alpha(T - T_0) + \delta(\mathbf{k} - \mathbf{q}_0) + \omega(\mathbf{k} - \mathbf{q}_0)^2 + \dots) \Phi, \quad (1)$$

where the function Φ transforms according to an irreducible (co-)representation induced by the little group of the bare propagation vector \mathbf{q}_0 and a summation over propagation vectors $\mathbf{k} - \mathbf{q}_0$ is implied. The experimentally observed \mathbf{q} lies on a line of symmetry [27]. Thus, the irreducible representations (irreps) of the little group belonging to \mathbf{q} and labeled U_i , $i = 1, \dots, 4$, have 1 degree of freedom, $\nu = 1$. Eventually, a commensurate order can be reached by a lock-in transition with propagation vector $\mathbf{q}_1 = (0, 1/2, 1/2)$. In this state, the order is described by irreps R_j , $j = 1, 2$, which are the degenerated versions of the four modes U_i owing to higher symmetry. The observation of propagation vector \mathbf{q} implies that the magnetically ordered state should be described by (1) with a small δ . The symmetry analysis for this incommensurate magnetic order belonging to irreps U_i (and, also, for irreps R_j) in Fe_{1+y}Te shows that there are $\mu > 1$ Lifshitz-type invariants, i.e., antisymmetric terms $\Phi_i \bar{\partial}_\xi \Phi_j \equiv \Phi_i \partial_\xi \Phi_j - \Phi_j \partial_\xi \Phi_i$ that couple different OP components [28].

The free energy expansion (1) can be extended to a phenomenological Dzyaloshinskii model by collecting the low-order invariant terms in OP components. Any magnetic ordering based on these modes must also be unconventional for the case of a mixed order that involves several propagation vectors as proposed, e.g., in terms of a plaquette ordering pattern [29,30]. However, the exposition here will be given by considering only one arm with a $\mathbf{q} = (0, q, 1/2)$ r.l.u. from the star of four propagation vectors belonging to modes with label U_i . This restriction is a reasonable simplification because the incommensurate magnetic order in Fe_{1+y}Te for $y \geq 0.11$ is linked to an orthorhombic distortion owing to strong spin-lattice couplings [20]. Thus, the modulation direction is determined by a strong anisotropy, and magnetic states as superposition

of states with several propagation vector directions appear unlikely to occur. The spin density is described by $\mathbf{S}^{(\pm)}(\mathbf{r}) = (\mathbf{a}^{(+)} \cos[\mathbf{q}_0 \cdot \mathbf{r}], \mathbf{a}^{(-)} \sin[\mathbf{q}_0 \cdot \mathbf{r}])$, with the local polarization given by three-component vectors $\mathbf{a}^{(\pm)}$ slowly varying on the scale of the lattice parameter. The free energy density for a modulated state of this type (in a Cartesian coordinate system with directions a, b, c parallel to the lattice vectors of the tetragonal crystal, and the propagation vector along b)

$$\begin{aligned} f = & A[(\nabla \mathbf{a}^{(+)})^2 + (\nabla \mathbf{a}^{(-)})^2] \\ & + \sum_{i=a,b,c} B_i [(\partial_i a_i^{(+)})^2 + (\partial_i a_i^{(-)})^2] + G \mathbf{a}^{(+)} \cdot \bar{\partial}_b \mathbf{a}^{(-)} \\ & + \sum_{k=a,c} \{D_k [a_k^{(+)} \bar{\partial}_k a_b^{(+)} + a_k^{(-)} \bar{\partial}_k a_b^{(-)}] \\ & + E_k [a_k^{(+)} \bar{\partial}_k a_b^{(-)} - a_k^{(-)} \bar{\partial}_k a_b^{(+)}]\} \\ & + \alpha(T - T_0)[(\mathbf{a}^{(+)})^2 + (\mathbf{a}^{(-)})^2] + \beta[(\mathbf{a}^{(+)})^2 + \mathbf{a}^{(-)})^2]^2 \\ & + \sum_{i=a,b,c} \{\kappa_i [a_i^{(+)} + a_c^{(-)}]^2 + \gamma_i [a_i^{(+)} - a_c^{(-)}]^2\}, \quad (2) \end{aligned}$$

describes isotropic and anisotropic exchange by coefficients A, B_i . The anisotropic terms are due to relativistic spin-orbit effects and should be weak. The next terms are $\mu = 5$ Lifshitz-type invariants. Importantly, the term with coefficient G is related to the presence of the incommensurate base magnetic mode. Invariants of this type originate from spin exchange [9,10]. They are not necessarily weak compared to the exchange term A . However, these terms cause a shift of the wave vector from \mathbf{q}_0 to \mathbf{q} . Therefore, in Fe_{1+y}Te , it must be weak enough so that a modulated state with propagation vector \mathbf{q} can be realized and the expansion according to (1) remains valid. The presence of such a term is corroborated by a strong temperature dependence of the magnitude $|\mathbf{q}|$ of the effective propagation vector, in agreement with the experimental observations on Fe_{1+y}Te [14,20,31,32]. The next terms with coefficients D_k, E_k originate from relativistic spin-orbit effects and are weak. These Dzyaloshinskii-Moriya (DM) couplings become operative because the incommensurate modulation breaks inversion symmetry and lowers the point group symmetry of the crystal from $4/mmm$ (D_{4h}) to $2mm$ (C_{2v}). The remaining homogeneous invariants correspond to the Landau expansion with bare transition temperature T_0 , and the mode coupling term β . Additional leading anisotropic terms with coefficients κ_i, γ_i are included to signal their crucial role for the thermodynamic stability of the modulated states and the lock-in transition. The explicit Landau-Ginzburg free energy demonstrates that a continuous phase transition according to Landau theory cannot take place in Fe_{1+y}Te for higher Fe contents where experiments observed a continuous transition into an incommensurate helixlike antiferromagnetic order [14–18,31,32]. The conundrum must be resolved by a closer experimental search for a precursor state above T_N .

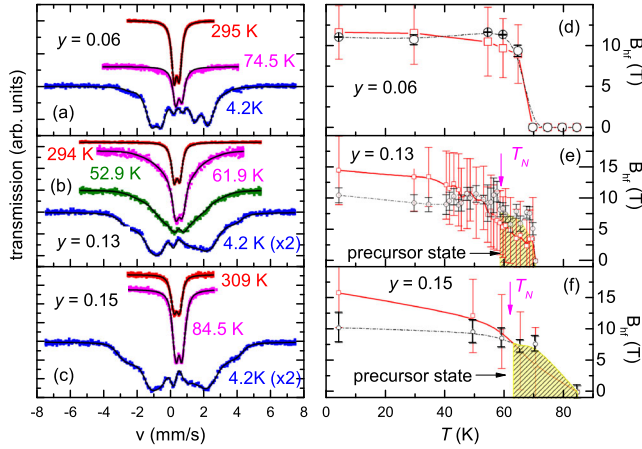


FIG. 1 (color online). Mössbauer spectra for Fe_{1+y}Te and fits (black curves) for $y = 0.06$ (a), 0.13 (b), and 0.15 (c). Corresponding T dependence of the magnetic hyperfine field B_{hf} for $y = 0.06$ (d), 0.13 (e), and 0.15 (f). Black circles and dashed lines correspond to the values obtained for pattern 2 (cf. text) while red lines and squares correspond to the average value of the magnetic hyperfine field distribution, which were obtained by the maximum entropy method (the error bars show standard deviations). Lines are guides to the eye.

For this purpose, we employ ^{57}Fe Mössbauer spectroscopy on polycrystalline powder samples of $\text{Fe}_{1.06}\text{Te}$, $\text{Fe}_{1.13}\text{Te}$, and $\text{Fe}_{1.15}\text{Te}$. These compositions were chosen because they fall in three different regimes of the phase diagram [14,15]. The ^{57}Fe Mössbauer spectra were recorded in the temperature range $T = 4.2\text{--}300$ K using a standard Mössbauer setup. ^{57}Co in a Rh matrix was used as a room temperature γ -ray source. The Mössbauer spectra were analyzed by diagonalizing the hyperfine Hamiltonian including electric quadrupole and magnetic hyperfine interactions combined with the maximum entropy method (MEM) in thin absorber approximation [27,33]. The experimentally observed Mössbauer spectra for selected temperatures are given in Figs. 1(a)–1(c). The spectra in the paramagnetic temperature region were analyzed using two patterns (subscripts 1 and 2). Each pattern contains a set of hyperfine parameters, namely the z component of the electric field gradient (EFG) V_{zz} , the isomer shift δ (with respect to α Fe) and the intensity I . In the magnetic temperature region, pattern 1 was described by a magnetic field distribution, which was obtained by MEM, while pattern 2 was described by a Lorentzian sextet pattern with a Gaussian-distributed magnetic field. The obtained relative intensities of pattern 1 (2) are 0.91 (0.09) for $y = 0.06$, 0.85 (0.15) for $y = 0.13$, and 0.77 (0.23) for $y = 0.15$. Therefore, it appears reasonable to assign pattern 1 to iron on the tetragonal sites and pattern 2 to the excess iron (see, also, Ref. [27]). The relative intensities were fixed over the whole temperature range. It turns out that both isomer shifts $\delta_{1,2}$ are of approximately equal value 0.472(5), 0.482(5), and 0.479(5) mm/s within error bars for $y = 0.06$, 0.13, and 0.15, respectively, at room temperature. With

decreasing temperature, the isomer shifts increase to values of $\delta_{1,2}^{y=0.06} \approx 0.63(1)$ mm/s, while for $y = 0.13$ and 0.15 a splitting is visible, as $\delta_1^{y=0.13} = 0.69(3)$ mm/s and $\delta_1^{y=0.15} = 0.67(3)$ mm/s are smaller than $\delta_2^{y=0.13} = 0.79(2)$ mm/s and $\delta_2^{y=0.15} = 0.74(3)$ mm/s at 4.2 K, respectively. At room temperature, the obtained values of $V_{zz,1}$ are 17.2(6) $\text{V}/\text{\AA}^2$, 18.4(1) $\text{V}/\text{\AA}^2$, and 17.2(6) $\text{V}/\text{\AA}^2$, while the second pattern has values of $V_{zz,2} = 32(1)$ $\text{V}/\text{\AA}^2$, 38(1) $\text{V}/\text{\AA}^2$, and 36(2) $\text{V}/\text{\AA}^2$ for $y = 0.06$, 0.13, and 0.15, respectively. With decreasing temperature, $V_{zz,1}$ increases slightly to values of 19.6(3) $\text{V}/\text{\AA}^2$, 21.0(3) $\text{V}/\text{\AA}^2$, and 20.5(5) $\text{V}/\text{\AA}^2$, while $V_{zz,2}$ increases to 40(1) $\text{V}/\text{\AA}^2$, 39.3(9) $\text{V}/\text{\AA}^2$, and 40(1) $\text{V}/\text{\AA}^2$ for $y = 0.06$, 0.13, and 0.15 at $T \approx 80$ K, respectively. The z component of the EFG was fixed for temperatures below 80 K. For $\text{Fe}_{1.06}\text{Te}$, the onset of the magnetic ordering is indicated by the appearance of a broadened sextet structure below 70 K. An abrupt onset of static magnetism can be seen from the temperature dependence of magnetic hyperfine field in Fig. 1(d). This behavior confirms the first-order magneto-structural transition in $\text{Fe}_{1.06}\text{Te}$. The magnetic field distribution of pattern 1 shows a single peak [27], which is consistent with a commensurate SDW and in good agreement with neutron diffraction measurements [14]. For samples $\text{Fe}_{1.13}\text{Te}$ and $\text{Fe}_{1.15}\text{Te}$, the temperature dependence of both the average value of this hyperfine field distribution as well as that obtained from pattern 2 are shown in Figs. 1(e) and 1(f). The corresponding field distributions [27] show a rectangular shape consistent with Ref. [34]. For the $\text{Fe}_{1.13}\text{Te}$ sample, a broadening of the spectral linewidth was already observed at 70.4 K indicating a quasistatic magnetic signal above $T_N = 57$ K. For $\text{Fe}_{1.15}\text{Te}$, a similar behavior is observed. i.e., a quasistatic magnetic signal is found starting from $T \approx 80$ K, which is clearly above $T_N = 62$ K. Upon increasing the amount of excess iron, the low-temperature magnitude of the magnetic hyperfine field remains constant for the excess iron while the average value of the hyperfine field distribution increases.

The salient point of the Mössbauer experiments is the observation of a quasistatic state at temperatures above the onset of LRO for the samples with $y \geq 0.11$ in Fe_{1+y}Te . The exact nature of this precursor state would require a quantitative treatment of the various parameters entering the Dzyaloshinskii model, Eq. (2). The required detailed assessment of spin-relativistic couplings and anisotropy effects is not available for Fe_{1+y}Te at present, and only qualitative statements can be made based upon the Dzyaloshinskii model. This model describes equilibrium magnetic states as minima of the magnetic free energy (2), which contain various types of modulated and localized magnetic states [9,11,13,35,36]. Depending on the character and strengths of the magnetic anisotropies, κ_i , γ_i , and B_i , and the DM couplings, the basic magnetic modulation with propagation in b direction is twisted into one-dimensional long-period spirals propagating within the ac plane. The pitch of these spiral modulations is given by $\Lambda_k \sim (A + B_k)/(2D_k)$ for propagation in $k = a, c$

directions. The spin structure in this state is modulated in two spatial directions with a short period, $\lambda = 2\pi/q$, of the SDW in b direction, while the polarization direction slowly twists over lengths $\Lambda \gg \lambda$ in a transverse direction, Fig. 2(a). This magnetic state can undergo a lock-in transition into a collinear magnetic structure, if the anisotropies become strong enough, see profiles in Fig. 2(d)(i)–(ii). The twisting of the basic collinear SDW transverse to the propagation vector \mathbf{q} yields an interpretation for those experimental results which describe helical or three-dimensional spin structures in Fe chalcogenides as inferred from neutron diffraction [14,20]. Simultaneous twisting in a and c directions driven by the terms D_a and D_c describes the double-twisted cores of a chiral Skyrmionic texture, Fig. 2(b), as earlier calculated for systems with C_{nv} symmetry [11,37,38]. However, the double-twisted configuration of \mathbf{a}^\pm is not topologically stable. The Skyrmionic strings display the “Alice behavior” [39,40], as they can be annihilated by a 180° phase shift of the primary modulation. A numerical analysis of two-dimensional textures, as described by (2) in the ac plane, revealed that the exchange anisotropy terms can stabilize a staggered assembly of half-Skyrmions, representing defective solitonic textures at temperatures above the onset of the one-dimensional spiral configuration [35,36]. Such textures are inhomogeneous, the amplitude $|\mathbf{S}|$ of the local OP varies strongly and passes through zero [41–44]. The temperature interval for these precursors is set by the magnitude of the Lifshitz invariants and must be sizable for Fe_{1+y}Te ($y \geq 0.11$) because of the exchange term G .

The most intriguing states described by (2) are three-dimensional solitons, Fig. 2(c). The cores of the multidimensional states, Figs. 2(b) and 2(c), can be considered as local superpositions of the one-dimensional profiles shown in Fig. 2(d)(iii): A modulation in propagation direction b , driven by the term with coefficient G , is combined with a double-twisting of the OP in transverse directions. These states are localized. Close to and above T_N , their amplitude may decay towards zero in the three spatial directions, Fig. 2(c).

Thermal and quenched disorder impede the formation of long-range ordered assemblies of such two-dimensional or three-dimensional solitons. Hence, liquidlike precursor states are formed. Multidimensional solitonic liquidlike states can more easily adjust to random collective pinning and are favored compared to long-period spirals for larger Fe excess. The phase diagram of Fe_{1+y}Te in Fig. 2(e) locates the liquidlike precursor state as found from the experiment. The diagram displays the expected qualitative features, in particular, an enlarged temperature range for the precursor state with increasing y and a tricritical Lifshitz point (L). Dynamic precursor fluctuations may explain observations of unconventional magnetic fluctuations in Fe_{1+y}Te with $y < 0.11$ by neutron scattering [22,31,32].

In conclusion, the incommensurate SDW order in Fe_{1+y}Te embodies elementary mechanisms to generate long-period, twisted, and multidimensionally modulated solitonic condensates. The experimental observation of a

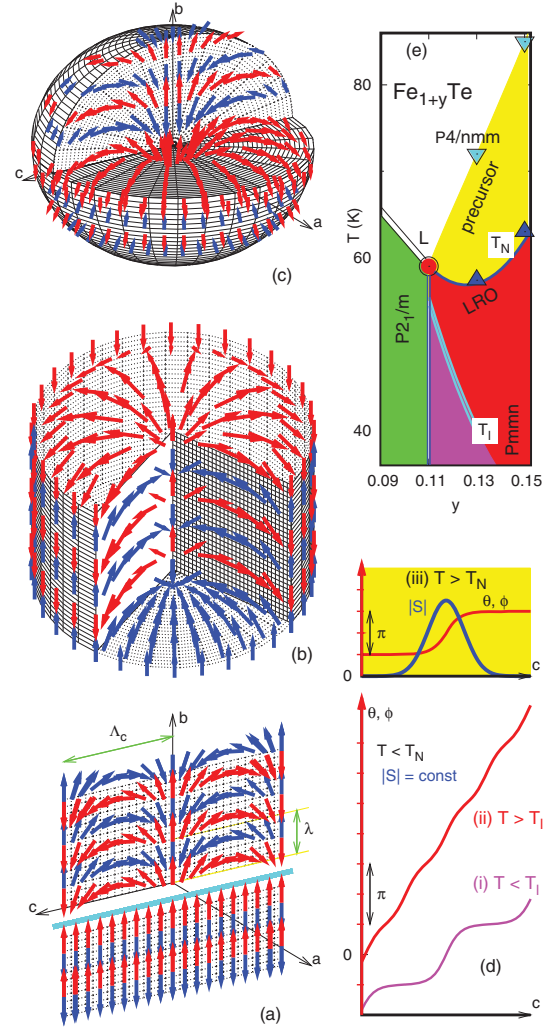


FIG. 2 (color). (a)–(c) Magnetic states described by the phenomenological Dzyaloshinskii model, Eq. (2). (The staggered atomic spin structure in c direction is represented by one sublattice only for clarity.) (a) A one-dimensional cycloidal spiral transverse (shown arbitrarily in c direction) to the propagating incommensurate spin-density wave along b (upper half) represents the LRO state. Lower half shows the commensurate collinear SDW state. (b) Two-dimensional Skyrmionic texture with a double-twisted core in the ac plane. (c) Three-dimensional solitonic state. (d) Profiles of one-dimensional states of modulated, $s_b \propto |S| \exp(i\phi)$, or twisted form, $(s_b, s_c) \propto |S| [\cos(\theta), \sin(\theta)]$: (i) Commensurate states with $|S|$ solitons below the lock-in transition. (ii) Incommensurate LRO. (iii) Isolated amplitude-modulated solitons that arise as fluctuations in the precursor state. (e) Schematic phase diagram for Fe_{1+y}Te . A spin-liquid state of solitons like those shown in (b) and (c) with amplitude modulation [(d)(iii)] precedes the incommensurate SDW-like state. Triangles mark experimental transition temperatures for the onset of the precursor and of T_N . At T_l a lock-in into a commensurate state occurs. Point “L” is a tricritical Lifshitz point of the spin system associated with structural phase transitions.

quasistatic magnetic order above T_N by Mössbauer spectroscopy confirms the existence of a liquidlike precursor state. The stabilizing mechanism of these textures is expected to be realized in various other systems with

incommensurate basic ordering modes, if they support multiple Lifshitz-type invariants. As the polarization of magnetic ordering vectors usually is rotatable and may belong to modes of different symmetry, spin-density wave systems are natural candidates for such behavior. Similar exotic behavior is also expected in magnetoelectric or magnetoelastic systems allowing for a coupling of an incommensurate mode with other secondary order parameters, because Lifshitz-type invariants do exist for almost all propagation vectors in the Brillouin zone with the exception of special symmetry points [10,45].

The authors thank A. N. Bogdanov, Yu. Grin, O. Stockert, and L. H. Tjeng for stimulating discussions. Financial support from Deutsche Forschungsgemeinschaft (within the Programs SPP1458 and GRK1621) is gratefully acknowledged.

*roessler@cpfs.mpg.de

- [1] P. A. Lee, N. Nagaosa, and X.-G. Wen, *Rev. Mod. Phys.* **78**, 17 (2006).
- [2] S. Nair, S. Wirth, M. Nicklas, J. L. Sarrao, J. D. Thompson, Z. Fisk, and F. Steglich, *Phys. Rev. Lett.* **100**, 137003 (2008).
- [3] M. B. Salamon and M. Jaime, *Rev. Mod. Phys.* **73**, 583 (2001).
- [4] X. Zhang, L. Yu, S. von Molnár, Z. Fisk, and P. Xiong, *Phys. Rev. Lett.* **103**, 106602 (2009).
- [5] D. C. Wright and N. D. Mermin, *Rev. Mod. Phys.* **61**, 385 (1989).
- [6] C. Pappas, E. Lelièvre-Berna, P. Falus, P. M. Bentley, E. Moskvín, S. V. Grigoriev, P. Fouquet, and B. Farago, *Phys. Rev. Lett.* **102**, 197202 (2009).
- [7] H. Wilhelm, M. Baenitz, M. Schmidt, U. K. Rößler, A. A. Leonov, and A. N. Bogdanov, *Phys. Rev. Lett.* **107**, 127203 (2011).
- [8] A. Barla, H. Wilhelm, M. K. Forthaus, C. Strohm, R. Ruffer, M. Schmidt, K. Koepnik, U. K. Rößler, and M. M. Abd-Elmeguid, *Phys. Rev. Lett.* **114**, 016803 (2015).
- [9] I. E. Dzyaloshinskii, *Zh. Eksp. Teor. Fiz.* **46**, 1420 (1964) [*Sov. Phys. JETP* **19**, 960 (1964)].
- [10] J. C. Tolédano and P. Tolédano, *The Landau Theory of Phase Transitions* (World Scientific, Singapore, 1987).
- [11] A. N. Bogdanov and D. A. Yablonskii, *Zh. Eksp. Teor. Fiz.* **95**, 178 (1989) [*Sov. Phys. JETP* **68**, 101 (1989)].
- [12] A. Michelson, *Phys. Rev. B* **18**, 459 (1978).
- [13] A. Bogdanov, Pis'ma, *Zh. Eksp. Teor. Fiz.* **62**, 231 (1995) [*JETP Lett.* **62**, 247 (1995)].
- [14] E. E. Rodriguez, C. Stock, P. Zajdel, K. L. Krycka, C. F. Majkrzak, P. Zavalij, and M. A. Green, *Phys. Rev. B* **84**, 064403 (2011).
- [15] S. Rößler, D. Cherian, W. Lorenz, M. Doerr, C. Koz, C. Curfs, Yu. Prots, U. K. Rößler, U. Schwarz, S. Elizabeth, and S. Wirth, *Phys. Rev. B* **84**, 174506 (2011).
- [16] I. A. Zaliznyak, Z. J. Xu, J. S. Wen, J. M. Tranquada, G. D. Gu, V. Solovyov, V. N. Glazkov, A. I. Zheludev, V. O. Garlea, and M. B. Stone, *Phys. Rev. B* **85**, 085105 (2012).
- [17] C. Koz, S. Rößler, A. A. Tsirlin, S. Wirth, and U. Schwarz, *Phys. Rev. B* **88**, 094509 (2013).
- [18] E. E. Rodriguez, D. A. Sokolov, C. Stock, M. A. Green, O. Sobolev, J. A. Rodriguez-Rivera, H. Cao, and A. Daoud-Aladine, *Phys. Rev. B* **88**, 165110 (2013).
- [19] C. Koz, S. Rößler, A. A. Tsirlin, D. Kasinathan, C. Börrnert, M. Hanfland, H. Rosner, S. Wirth, and U. Schwarz, *Phys. Rev. B*, **86**, 094505 (2012).
- [20] W. Bao *et al.*, *Phys. Rev. Lett.* **102**, 247001 (2009).
- [21] S. Li *et al.*, *Phys. Rev. B* **79**, 054503 (2009).
- [22] I. A. Zaliznyak, Z. Xu, J. M. Tranquada, G. Gu, A. M. Tsvelik, and M. B. Stone, *Phys. Rev. Lett.* **107**, 216403 (2011).
- [23] D. Fobes *et al.*, *Phys. Rev. Lett.* **112**, 187202 (2014).
- [24] C. Stock, E. E. Rodriguez, O. Sobolev, J. A. Rodriguez-Rivera, R. A. Ewings, J. W. Taylor, A. D. Christianson, and M. A. Green, *Phys. Rev. B* **90**, 121113(R) (2014).
- [25] M.-C. Ding, H.-Q. Lin, and Y.-Z. Zhang, *Phys. Rev. B* **87**, 125129 (2013).
- [26] S. Ducatman, R. M. Fernandes, and N. B. Perkins, *Phys. Rev. B* **90**, 165123 (2014).
- [27] See Supplemental Material at <http://link.aps.org/supplemental/10.1103/PhysRevLett.115.177203> for symmetry analysis, derivation of the Dzyaloshinskii model, and data analysis of Mössbauer spectra.
- [28] The violation of the Lifshitz condition has been checked with the help of the ISOTROPY software, cf. H. T. Stokes, D. M. Hatch, and B. J. Campbell (2007), <http://stokes.byu.edu/isotropy.html>; see, also, Supplemental Material [27].
- [29] S. Ducatman, N. B. Perkins, and A. Chubukov, *Phys. Rev. Lett.* **109**, 157206 (2012).
- [30] M. Enayat *et al.*, *Science* **345**, 653 (2014).
- [31] C. Stock, E. E. Rodriguez, M. A. Green, P. Zavalij, and J. A. Rodriguez-Rivera, *Phys. Rev. B* **84**, 045124 (2011).
- [32] D. Parshall, G. Chen, L. Pintschovius, D. Lamago, Th. Wolf, L. Radzihovsky, and D. Reznik, *Phys. Rev. B* **85**, 140515 (2012).
- [33] The natural line width of the 57-Fe transition is 0.097 mm/s. A new radioactive 57-Co source usually has a line width of 0.11–0.12 mm/s which increases slowly to higher values of about 0.15 mm/s after some time. As the source was not new, the line width of 0.13 mm/s is considered to be related to the source and confirms a homogeneous behavior of our samples.
- [34] A. Błachowski, K. Ruebenbauer, P. Zajdel, E. E. Rodriguez, and M. A. Green, *J. Phys. Condens. Matter* **24**, 386006 (2012).
- [35] U. K. Rößler, A. N. Bogdanov, and C. Pfleiderer, *Nature (London)* **442**, 797 (2006).
- [36] A. A. Leonov, Thesis, University of Technology, Dresden, 2012, http://www.qucosa.de/fileadmin/data/qucosa/documents/8382/Thesis_Leonov.pdf; see, also, A. A. Leonov, U. K. Rößler, and A. N. Bogdanov, arXiv:1001.1292.
- [37] A. N. Bogdanov and A. Hubert, *J. Magn. Magn. Mater.* **138**, 255 (1994).
- [38] A. N. Bogdanov, U. K. Rößler, M. Wolf, and K.-H. Müller, *Phys. Rev. B* **66**, 214410 (2002).
- [39] A. S. Schwarz, *Nucl. Phys.* **B208**, 141 (1982).
- [40] U. Leonhardt and G. E. Volovik, *JETP Lett.* **72**, 46 (2000).
- [41] M. Yamashita, *J. Phys. Soc. Jpn.* **56**, 1414 (1987).
- [42] B. Schaub and D. Mukamel, *Phys. Rev. B* **32**, 6385 (1985).
- [43] U. K. Rößler, A. A. Leonov, and A. N. Bogdanov, *J. Phys. Conf. Ser.* **200**, 022029 (2010); **303**, 012105 (2011).
- [44] O. Janson, I. Rousochatzakis, A. A. Tsirlin, M. Belesi, A. A. Leonov, U. K. Rößler, J. van den Brink, and H. Rosner, *Nat. Commun.* **5**, 5376 (2014).
- [45] H. T. Stokes and D. M. Hatch, *Phys. Rev. B* **30**, 4962 (1984).